LBL-11314 c. 2

Lawrence Berkeley Laboratory
UNIVERSITY OF CALIFORNIA

Materials & Molecular
Research Division

Presented at the Annual Meeting of the Materials Research Society, Boston, MA, November 17-20, 1980

# A MÖSSBAUER STUDY OF MICROSTRUCTURAL AND CHEMICAL CHANGES IN FE-9NI STEEL DURING TWO-PHASE TEMPERING

B. Fultz and J.W. Morris, Jr.

November 1980

LAWRENCE
BERKELEY LABORATORY
MAR 3 1981
LIBRARY AND
DOCUMENTS SECTION

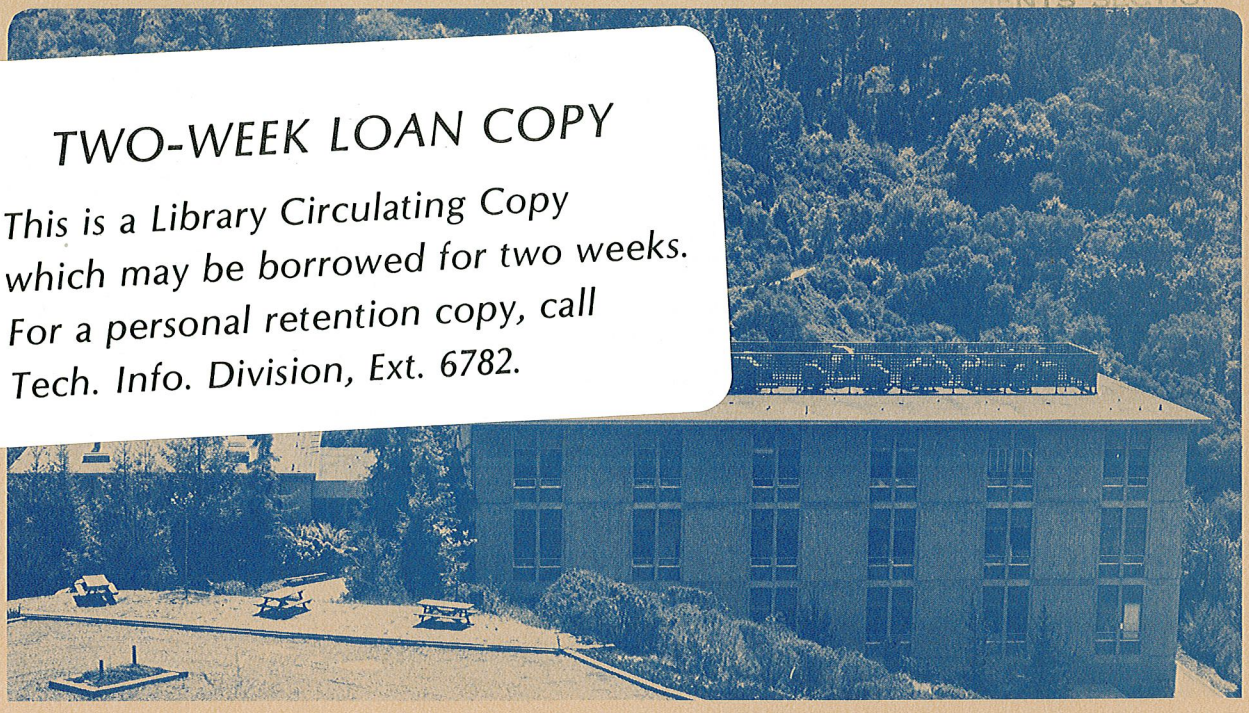

TWO-WEEK LOAN COPY

This is a Library Circulating Copy
which may be borrowed for two weeks.
For a personal retention copy, call
Tech. Info. Division, Ext. 6782.

LBL-11314 c. 2

Prepared for the U.S. Department of Energy under Contract W-7405-ENG-48

# A MÖSSBAUER STUDY OF MICROSTRUCTURAL AND CHEMICAL CHANGES IN FE-9NI STEEL DURING TWO-PHASE TEMPERING

B. FULTZ AND J. W. MORRIS, JR.
Materials and Molecular Research Division, Lawrence Berkeley Laboratory and the Department of Materials Science and Mineral Engineering, University of California, Berkeley, California 94720, USA

## ABSTRACT

Two-phase tempering of martensitic Fe-9Ni steel serves to enhance the low temperature toughness and forms austenite precipitates in this material. Hyperfine field effects in Fe-Ni alloys were systematized so that tempering induced chemical composition changes in the martensite could be quantified by Mössbauer spectrometry. The kinetics of segregation of alloy elements from the martensite into the fresh austenite can be determined simultaneously with the amount of austenite which has formed.

## INTRODUCTION

Fe-9Ni steel with the commercial "quenched and tempered" heat treatment has seen increasing application as a structural material in cryogenic temperature environments. The notch toughness of this material at low temperatures is dramatically improved after tempering the martensitic quenched material for one hour or so at 600°C. Transmission electron microscopy [1,2] has shown that during this tempering treatment crystals of austenite, $\gamma$ phase, form between the crystals of tempered martensite, $\alpha_t$ phase.

Through study of the tempering-induced microstructural changes we hope to eventually clarify the mechanism of the low temperature mechanical property improvements in Fe-9Ni steel. Any such fundamental study must quantify the amount of precipitated $\gamma$ phase and also determine the alloy chemistry of the $\gamma$ and $\alpha_t$ phases because the chemical composition of the $\gamma$ phase will influence its formation and stability against the martensite transformation. During tempering the characteristic diffusion distances of Mn, Cr, and Si in the $\alpha$ phase are only a few thousand angstroms or less, so we expect the kinetics of chemical segregation to play an important role in the $\gamma$ phase precipitation process. A method for studying both the amount of $\gamma$ phase which has precipitated and the extent of alloy element segregation to the $\gamma$ or $\alpha$ phases is necessary in our research program, but the small dimensional scale (<1μm) and the small fraction of precipitated $\gamma$ phase (a few percent) makes this precipitation process and associated chemical segregation effects amenable to study by only a few experimental techniques.

By simultaneously quantifying the extent of this precipitation reaction and the associated kinetics of alloy element segregation, Mössbauer spectrometry is serving as a unique and valuable tool in materials science. The method of phase analysis by Mössbauer spectrometry uses the fact that $Fe^{57}$ nuclei in the paramagnetic $\gamma$ phase see no hyperfine field and exhibit a single absorption peak near zero Doppler shift energy, whereas peaks from $Fe^{57}$ nuclei in the ferromagnetic $\alpha$ phase are well removed from zero Doppler shift energy because of the large hyperfine magnetic field and the nuclear Zeeman effect. We refer to the literature for a description of this method of phase analysis [3], but in the work reported here we will describe how Mössbauer spectrometry proves

This manuscript was printed from originals provided by the author.

efficient in simultaneously determining chemical changes in the α phase which accompany the precipitation of the γ phase during tempering. Such chemical information is obtained from perturbations in the hyperfine magnetic fields at $Fe^{57}$ nuclei which are situated next to alloy element atoms. We have systematized the perturbations in $Fe^{57}$ hyperfine magnetic fields in quenched, α phase Fe-Ni binary alloys and in Fe-Ni-X* ternary alloys so that this information could be used to quantitatively determine the chemical composition of the α phase in these materials. We then tempered these quenched alloys to form some γ phase and followed the alloy element segregation process by determining the chemical changes in the α phase. These chemical changes in the α phase were small, so a difference spectrum procedure was employed to compare the Mössbauer spectra before and after tempering.

## EXPERIMENTAL

In the study of alloy element effects on room temperature Mössbauer spectra we used a constant acceleration transmission geometry spectrometer with an Austin Science Associates electromechanical drive, a Kr and $CO_2$ filled proportional counter, and a microcomputer setup for 1024 channel multichannel scaling. In many experiments small peak shifts were measured, so we closely monitored the performance of the Doppler drive unit by collecting a spectrum from the same pure iron foil after alternate runs. It was found that drive stabilities of better than 0.1 data channels at the $I = \pm^1/_2 \rightarrow I = \pm^3/_2$ absorption peaks occurred for periods of up to two weeks. However, two spectra taken at different times for which the $I = +^1/_2 \rightarrow I = +^3/_2$ peak was shifted by 0.4 data channels, for example, could be compared on the same Doppler shift energy axis by adding the data channels together in pairs. In this example 25% of the $n+1^{st}$ data channels were added to the $n^{th}$ data channels to shift one spectrum downwards by 0.2 data channels, and 25% of the $n-1^{st}$ data channels were added to the $n^{th}$ data channels to shift the other spectrum upwards by 0.2 data channels. The data of Fig. 3 and Fig. 4 were processed in this way.

The 100 mCi $Co^{57}$ in Pd radiation source caused the proportional counter to show some evidence of saturation behavior. The counter recovery time was comparable to the time spent scanning the absorption peaks, and a problem could be seen for 25 μm natural iron absorbers which exhibited a large dip in count rate at the Mössbauer peaks. In these specimens an asymmetrical distortion of the absorption peaks could be readily found by comparing peak shapes of the two spectra taken with opposite accelerations of the Doppler drive. To suppress this distortion, the single channel analyzer window was set much wider than the detector energy resolution for 14.4 keV γ-rays, and very thin (5μm) specimens were used. The very thin specimens also ensured that absorber thickness distortion effects could be neglected.

Alloys were prepared by melting 99.99% purity components in a vacuum furnace under He backpressure. The furnace cooling rate was sufficient to ensure that the high temperature γ phase transformed to α phase martensitically without the chemical segregation effects associated with α phase precipitation. Negligible weight losses were found after melting, and no surface reactions were observed for any of the melted alloys, so chemical compositions were determined and controlled by the weights of the component elements. After cold rolling to 50 μm, the foils were prepared by heating 50-100°C into the γ phase region of the Fe-Ni phase diagram for 10 minutes in an inert atmosphere and water quenched. The quenched foils were then chemically polished to their final thickness. Before tempering, the same foil used for collecting the quenched α phase spectrum was sealed in an evacuated pyrex ampule with a low Ar backpressure. No surface oxidation was observed after tempering.

---

*"X" was one of the elements Mn, Cr, Si, or C which are alloy additions of <1% concentration in commercial Fe-6Ni and Fe-9Ni steel.

## MÖSSBAUER SPECTROMETRY RESULTS AND INTERPRETATION

Ni Analysis. In α phase Fe-Ni alloys, the dependence of the isomer shift on the concentration of Ni is small (See Fig. 1). At lower Ni concentrations we have found an isomer shift of 0.0035 mm/sec/%Ni, larger than the 0.0023 mm/sec/%Ni determined by Vincze and Campbell [4], but a shift of 0.032 ± 0.003 mm/sec was found for our Fe-12.0 at.% Ni alloy. We believe that we have observed a very small electric quadrupole splitting in this alloy which is twice as large as that reported for pure α-phase iron [5].

Much larger and easier to measure changes in Mössbauer spectra with changes in Ni concentration arise from hyperfine magnetic field effects. An Fe-9% Ni alloy is not a dilute solution of Ni in Fe, and there is a high probability than an $Fe^{57}$ nucleus will experience perturbations in its hyperfine magnetic field from several adjacent Ni atoms. The perturbation from each Ni atom is not large so no structure is resolvable in Mössbauer peaks of Fe-Ni alloys. Nevertheless, for quantitative analyses of Ni composition it is sufficient to consider the change in the numerically calculated first moments and the change in the full width at half maximum (FWHM) of the $I = \pm^1/_2 \rightarrow I = \pm^3/_2$ absorption peaks as a function of Ni composition. From Fig. 1 we see that when an α phase Fe-9Ni alloy experiences a small decrease in Ni concentration the decrease in the FWHM of the $I = \pm^1/_2 \rightarrow I = \pm^3/_2$ peaks, the decrease in isomer shift, and the decrease in the mean hyperfine magnetic field will all be proportional to the Ni concentration change. We have shown that when the shift in the first moment and the increase in the FWHM of a family of normalized lorentzian functions are both proportional to composition, and in the case when the changes in all the $n^{th}$ moments of a family of peaked curves scale by a factor proportional to the composition raised to the $n^{th}$ power, the height from valley to peak of a difference spectrum of two such peaked functions generated for slightly different compositions will be closely proportional to the composition difference.

The $I = \pm^1/_2 \rightarrow I = \pm^3/_2$ peaks from Fe-<10 at.% Ni alloys fulfill the criteria for the proportionality of difference spectrum heights to small Ni composition changes. An Fe-8.8 at.% Ni alloy foil was tempered for 1 hr at 600°C to produce 1½% γ phase (see the small peak around channel 124 in Fig. 2). The difference of spectra taken from this material before and after tempering (also shown in Fig. 2) gives the same shape around the $I = \pm^1/_2 \rightarrow I = \pm^3/_2$ peak positions as for the normalized Fe-6.0 at.% Ni and Fe-8.8 at.% Ni alloys shown in Fig. 3, but with only about 1/5 the relative intensity. The proportionality between difference spectrum height and Ni concentration change indicates that the Ni content of the α-phase was reduced by 1/5 x (8.8-6.0)% ≃1/2% after tempering. A Ni content of 33% in the 1½% γ-phase is hence implied. This is larger than 21% Ni in the γ phase as predicted from the Fe-Ni phase diagram but shows the predicted trend. In Fe-Ni-X ternary alloys such differential evidence of Ni depletion in the α phase after tempering could be found on the high Doppler shift energy side of the $I = \pm^1/_2 \rightarrow I = \pm^3/_2$ absorption peaks (see Fig. 5), but the difference on the low Doppler shift energy side was dominated by the hyperfine magnetic field effects of the X element. These X element hyperfine field effects were first found in a commercial Fe-Ni alloy steel by Kim and Schwartz [6] who suggested that they arose from the small number of $Fe^{57}$ nuclei near C atoms.

Mn, Cr, Si, and C Analysis. Early experiments by Wertheim et al. [7] and succeeding studies [4,8,9] have examined the hyperfine magnetic field effects induced at $Fe^{57}$ nuclei by moderately dilute concentrations of alloy elements in α phase Fe. There are many probable local environments for an $Fe^{57}$ nucleus in a non-dilute solid solution, so there is often a problem with the uniqueness of the empirical parameters which specify hyperfine magnetic field changes for $Fe^{57}$ nuclei which are situated near X element atoms. Less ambiguous chemical information may be obtained for dilute solutions of X in Fe. Assuming that

the martensitic quenched material is a random solid solution, the Mössbauer spectrum of an Fe-dilute X alloy should show a main peak from $Fe^{57}$ nuclei whose hyperfine fields are largely unaffected by X atoms and additional satellite absorption peaks from $Fe^{57}$ nuclei which see hyperfine magnetic field perturbatations from one (rarely two) X atom neighbors. The ratio of satellite intensity to total peak intensity should be determined as in [7] by the binomial probability distribution but in dilute alloys this ratio will be nearly equal to the concentration of X times the total number of nearest neighbor sites around an $Fe^{57}$ nucleus at which an X element atom will produce a strong hyperfine magnetic field perturbation.

The satellite intensity for our Fe-0.77 at.% Mn alloy (Fig. 4) is revealed by the difference spectrum method described below. The 6+% satellite to total peak integrated intensity ratio found with this difference spectrum indicates that there are 9±2 sites around each Mn atom at which an $Fe^{57}$ nucleus will experience a substantial perturbation in its hyperfine magnetic field. This would appear to correspond to the first nearest neighbor shell in the bcc structure which contains 8 atoms.

In our analysis of Fe-Ni-X materials, we assumed that their Mössbauer peaks also consisted of a main peak, which had the same shape as the peak from an Fe-Ni binary alloy, and an additional satellite peak from $Fe^{57}$ nuclei which experienced a large perturbation in their hyperfine magnetic fields due to the presence of an adjacent X element atom. The difference spectrum procedure used to extract the satellite peak intensity did not start with peaks of equal integrated intensity; the area enclosed by an Fe-Ni peak was always less than the area of the corresponding peak of the Fe-Ni-X spectrum by an amount equal to the satellite peak area. In addition to this normalization problem, and additional parameter for the difference spectrum method was necessary in the case of Fe-Ni-X ternary alloys and Fe-X binary alloys as well. The main absorption peak from these materials is due to $Fe^{57}$ nuclei which are out of range of the strong local electron spin disturbances of the alloy element atoms, but this peak is known to exhibit a hyperfine magnetic field change of a small amount proportional to the X element concentration. Thus in preparing the difference spectra, it was necessary to vary both the shift of the main peak and the peak area normalization.

We expect that there will be little intensity due to the satellite peak on the high Doppler shift energy side of the absorption peaks of Fe-Ni-X alloys because Mn, Cr, and Si are known to induce hyperfine magnetic field perturbations at neighboring $Fe^{57}$ nuclei which are large and negative in $\alpha$-phase Fe. For a given main peak shift, the tails on the high Doppler shift energy side of Fe-Ni-X and Fe-Ni Mössbauer peaks were least squares fit, and the peak normalization which gave the best fit was used for generating the difference spectrum. In this way, other values of peak shifts were then used to generate difference spectra, and the best value of peak shift was chosen on the basis of giving a smooth difference spectrum baseline in the region of the tip of the main part of the absorption peak. With our assumption of the Fe-Ni-X peaks being composed of an Fe-Ni component and a satellite component, a properly normalized and shifted Fe-Ni-X peak should match well the Fe-Ni peak on the high Doppler shift energy side, and then smoothly drop below the Fe-Ni peak intensity as the peaks are examined from high to low Doppler shift energy. Dips or sudden rises in the baseline of the difference spectra would hence not be expected and were grounds for rejecting most difference spectra. The least squares fitting procedure gave results for the satellite peak intensity which were within ~2% of the satellite intensities found in the difference spectra generated with the authors' discretion; this discrepancy was, in part, attributed to variations in the asymmetric peak distortion described in the experimental section.

Difference spectra of quenched Fe-Ni-0.75 at.% Mn and Fe-Ni alloys are shown in Fig. 4. The satellite peak intensity was consistently larger than predicted

for hyperfine field perturbations from Mn atoms only in the first nearest neighbor shell. Based on these integrated intensities there appear to be 13 ± 2 neares neighbor sites around each Mn atom at which an $Fe^{57}$ nucleus will experience a strong perturbation in its hyperfine magnetic field in Fe-3.0 at.% Ni and Fe-6.0 at.% Ni alloys. No such difference in hyperfine field effects were found for Cr in Fe, Fe-3.0 at.% Ni or Fe-6.0 at.% Ni hosts for which there are 14 ± 2 strongly perturbing sites around an $Fe^{57}$ nucleus. We believe that Cr and Mn neighbor satellite peaks extracted from the broadened peaks of Fe-9Ni and Fe-12Ni hosts showed an intensity increase which indicates 20 ± 5 strongly perturbing neighbor sites. A quantitative basis has now been provided for determination of small Mn and Cr concentration changes in α phase Fe-Ni-X alloys by examination of spectrum intensity differences on the low Doppler shift energy sides of the Mössbauer absorption peaks.

Figure 5 shows transmission Mössbauer spectra of an Fe-8.8 at.% Ni-0.76 at.% Mn foil which were taken before and after 3½ hrs. tempering at 600°C to produce 6% γ phase. The difference spectrum around the $I = \pm^1/_2 \rightarrow I = \pm^3/_2$ (and $I = \pm^1/_2 \rightarrow I = \pm^1/_2$) absorption peaks shows a change on the high Doppler shift energy side which indicates a reduction of ~0.6 at.% Ni. After roughly correcting the intensity of the satellite peaks on the low Doppler shift energy side for this Ni reduction, we find a decrease in Mn neighbor satellite intensity which indicates a loss of ~0.2 at.% Mn from the α phase. The metastable γ phase was then transformed martensitically to α phase by quenching the foils in liquid nitrogen and lightly hammering them at room temperature. The difference spectrum of Fig. 5c shows a transformation of half of the γ phase and a simultaneous gain in average Ni content of the α phase. No change in Mn content of the α phase is evident, however. Very similar tempering effects were found in Mössbauer spectra of Fe-9Ni-C, Fe-9Ni-Si, and Fe-9Ni-Cr alloys. The Si, Cr, and especially the C segregation processes appear to occur more readily than the Mn segregation.

## CONCLUSIONS

After hyperfine magnetic field effects are systematized so that chemical composition changes in the α phase can be quantified by Mössbauer spectrometry, a difference spectrum method can be used to detect small chemical composition changes in α phase Fe-Ni-X alloys. This procedure is being used to determine the kinetics of alloy element segregation from martensite into the austenite precipitated during a tempering treatment.

## ACKNOWLEDGEMENT

This work was supported by the Division of Materials Sciences, Office of Basic Energy Sciences, U.S. Department of Energy under contract No. W-7405-Eng-48.

## REFERENCES

1. T. Ōoka et al., Jour. Japan Inst. Metals 30, 442 (1966).

2. C. K. Syn, B. Fultz, and J. W. Morris, Jr., Met. Trans. A 9, 1635 (1978).

3. L. H. Schwartz in: Applications of Mössbauer Spectroscopy Vol. I, chapter 2, R. Cohen ed. (Acad. Press, N.Y. 1976).

4. I. Vincze and I. A. Campbell, Jour. Phys. F 3, 647 (1973).

5. J. J. Spijkerman et al., Phys. Rev. Lett. 26, 323 (1971).

6. K. J. Kim and L. H. Schwartz, Mater. Sci. Eng. 33, 5 (1978).

7. G. K. Wertheim et al., Phys. Rev. Lett. 12, 24 (1964).

8. M. B. Stearns, J. Appl. Phys. 36, 913 (1965).

9. W. E. Sauer and R. J. Reynik, J. Appl. Phys. 42, 1604 (1971).

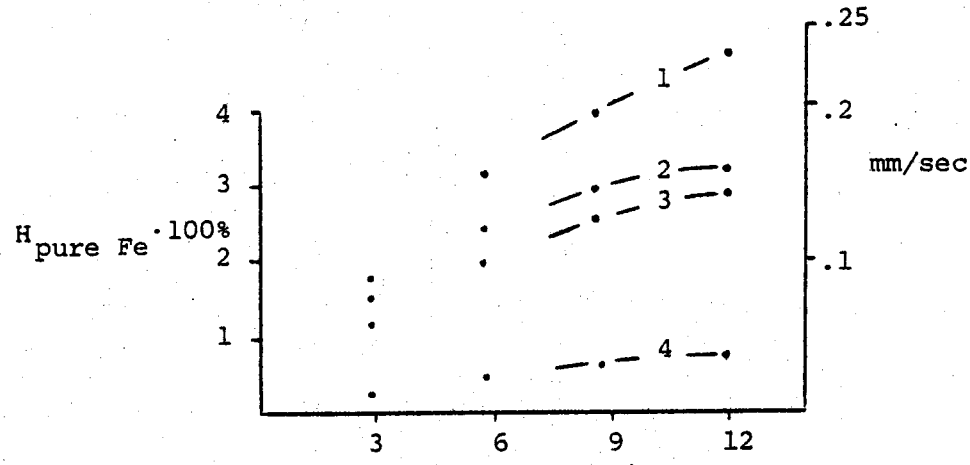


Fig. 1

1 Δ FWHM of $I=-1/2 \rightarrow I=-3/2$ peak (mm/sec)
2 Δ FWHM of $I=+1/2 \rightarrow I=+3/2$ peak (mm/sec)
3 $\langle H \rangle - \langle H_{pure\ Fe} \rangle$ ($H_{Fe} \cdot 100$ %)
4 Isomer shift with respect to pure Fe (mm/sec)

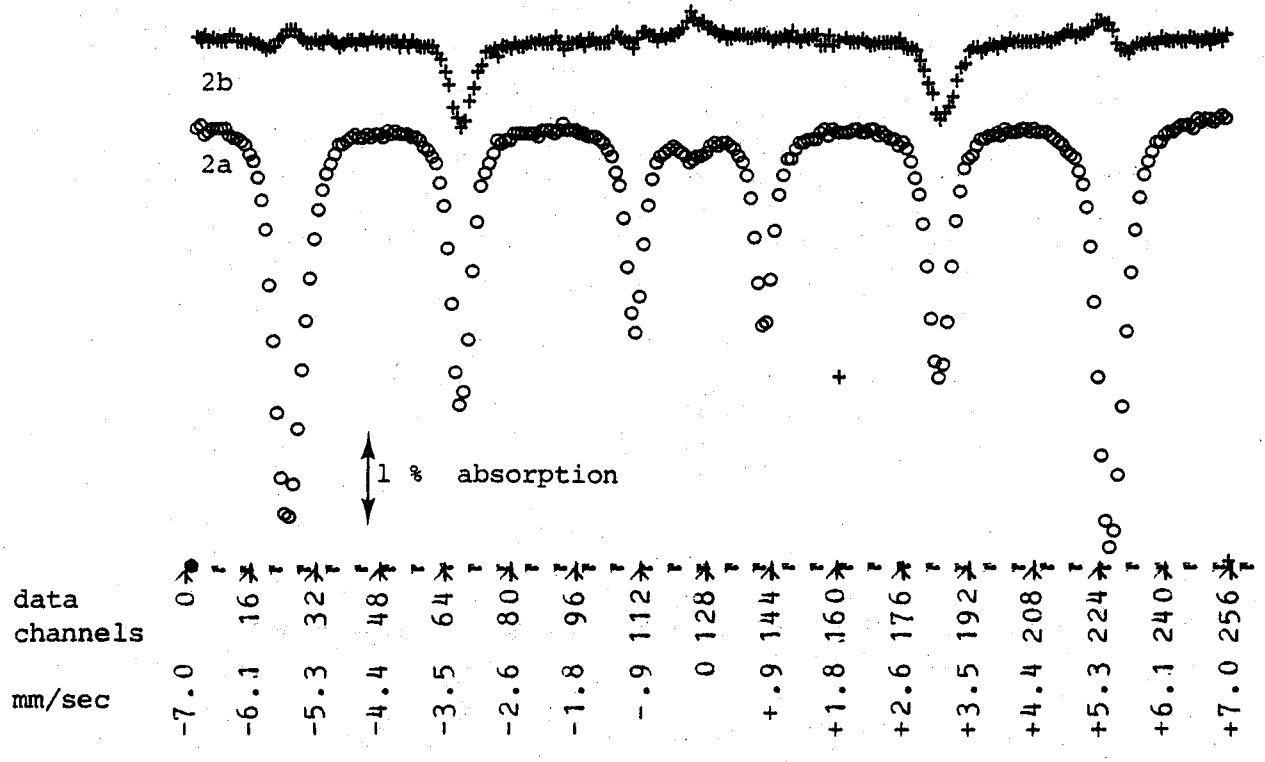


Fig. 2a o Fe-8.8 at.% Ni tempered 1 hr at 600°C
2b + difference of quenched Fe-8.8 at.% Ni spectrum (not shown) minus spectrum of 2a (same absorption scale)

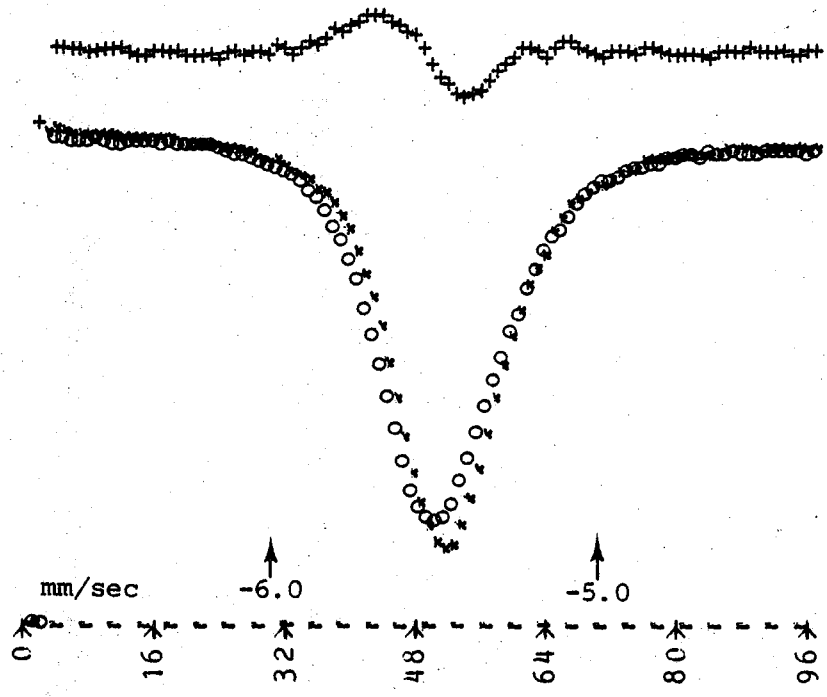


Fig. 3 o quenched Fe-8.8 at.% Ni
* quenched Fe-6.0 at.% Ni
\+ difference spectrum of above ( * - o ) (same absorption scale)

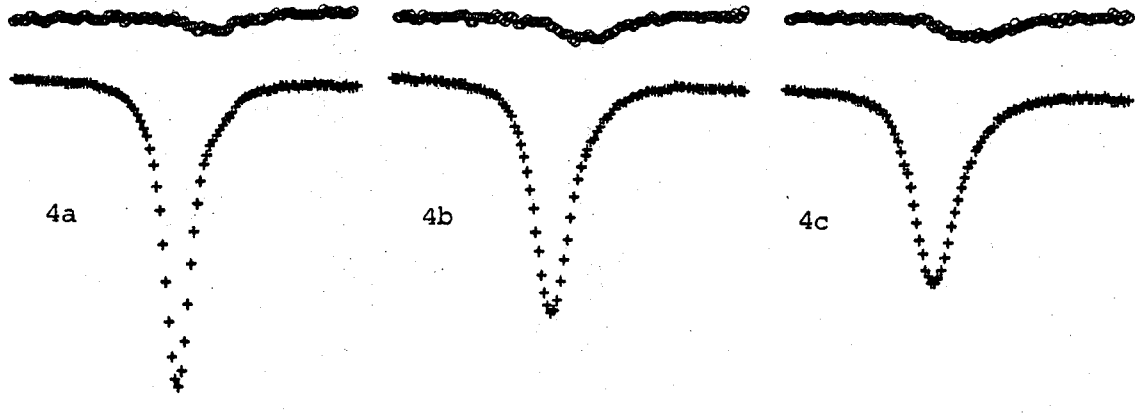


Fig. 4 Normalized spectra:
4a + quenched Fe-0.74 at.% Mn binary alloy spectrum
o difference spectrum of + spectrum minus pure Fe spectrum
4b + quenched Fe-3.0 at.% Ni-0.76 at.% Mn spectrum
o difference spectrum of + spectrum minus Fe-3.0 at.% Ni spectrum
4c + quenched Fe-6.0 at.% Ni-0.76 at.% Mn spectrum
o difference spectrum of + spectrum minus Fe-6.0 at.% Ni spectrum

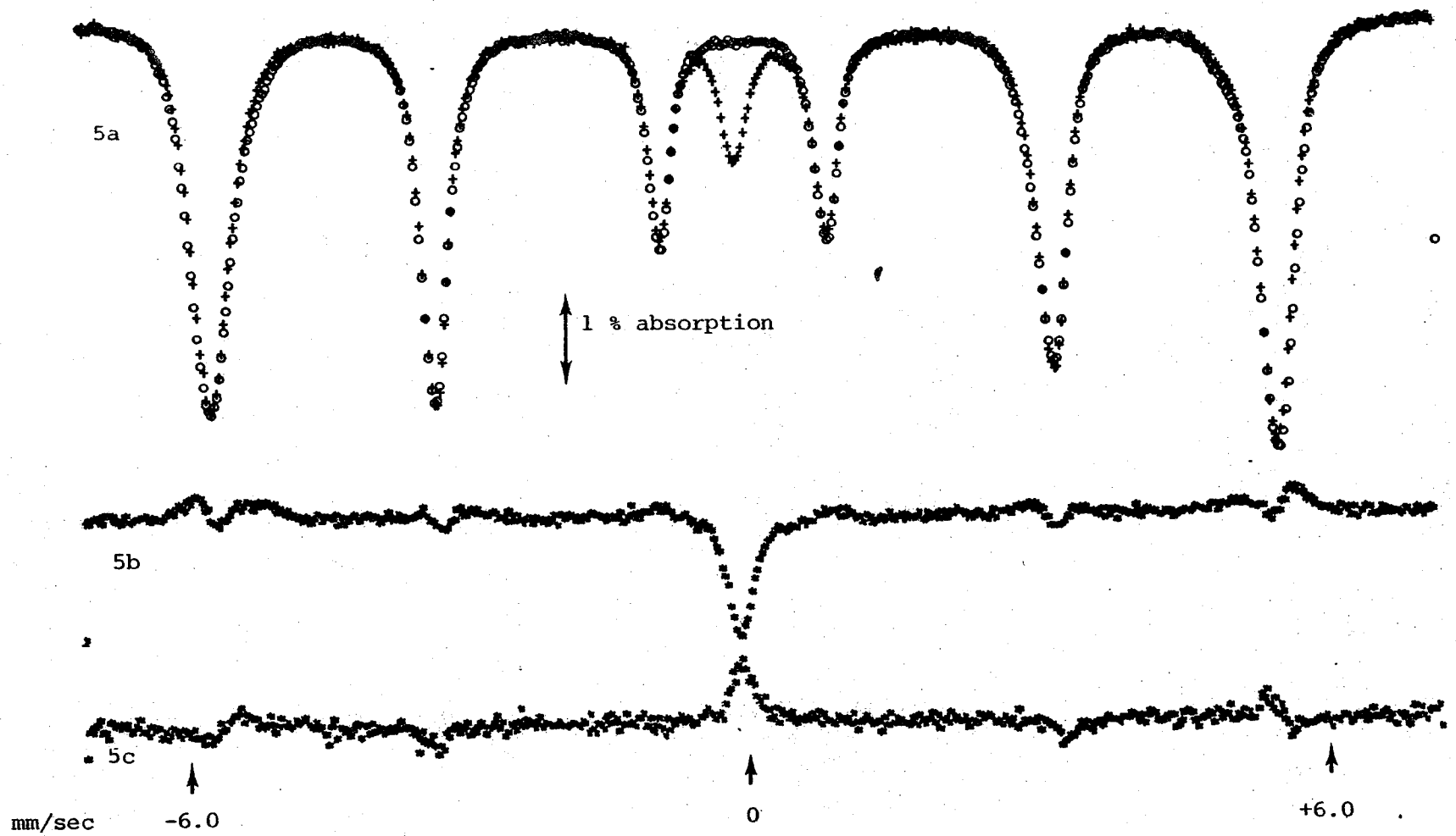


Fig. 5a o quenched Fe-8.8 at.% Ni-0.74 at.% Mn ; + same foil after tempering 3½ hrs at 600°C
5b * difference spectrum of spectra in 5a ( + - o )
5c * difference spectrum for same foils of 5a+ before and after hammering and quenching to 77°K
(after - before)

(same absorption scale for all spectra in Fig. 5)